

# Overview on the installation of a U-Oscillating Water Column breakwater in the Port of Salerno

Felice Arena, Alessandra Romolo, Giovanni Malara, Valentina Laface,  
Elena Valentino, Francesco Messina

**Abstract**— This article describes the characteristics of a U-Oscillating Water Column plant, named also REWEC3 (REsonant Wave Energy Converter), that will be installed in the Port of Salerno (Italy). The objective of the infrastructure is to enlarge the port basin area by taking advantage of the most recent developments in the field of caisson breakwaters. A general overview on the geometrical characteristics of the plant is given in conjunction with a description of its introduction in the existing port layout. Next, an example of expected plant performance is described by utilizing relevant Monte Carlo data. The article shows that the plant may absorb about 60-80% of the incident wave energy in certain sea states available in the location under study.

**Keywords**— U-OWC, harbour, prototype.

## I. INTRODUCTION

WAVE energy converters were developed and tested by several research teams and the development stage of some of them reached the prototypal stage. This is the case for the Oscillating Water Column (OWC) devices that, since the pioneering tests of Yoshio Masuda [1], have been tested in various areas

worldwide. For instance, OWCs were tested in the Sea of Japan [2], in India [3], in Europe at Pico Island (Azores, Portugal) [4] and at Islay (Scotland, UK) [5], and in other locations worldwide (see Ref. [6] for a broad perspective on the topic).

This article deals with the description of a full scale OWC plant soon under construction. Specifically, the article describes the main characteristics of a port infrastructure equipped with a U-Oscillating Water Column (U-OWC) (also known as REWEC3) wave energy converter. This particular device was proposed by Boccotti [7], [8] and further investigated by Arena et al. [9], [10]. As classical OWCs, it is composed by a partially closed air chamber, with a small orifice connected to the atmosphere, located on a water column which in turn is connected to the open wave field. In addition, the U-OWC includes a small vertical duct connecting the water column to the sea. Such a small element is used for tuning the eigenperiod of the system to a desired period. Thus, limiting the use of devices for phase control [11].

The very first U-OWC prototype was constructed and installed in the port of Civitavecchia (Rome, Italy) [12]. It was a large infrastructure composed by 17 caissons, each equipped with 8 independent U-OWC chambers. This plant was the objective of several articles that described the expected performances, produced power and the outcomes of a monitoring activity. The main result of this experimental campaign was the assessment of the reliability of the mathematical models utilized for estimating the U-OWC response and the demonstration of its reliability as wave energy absorber/converter [13], [14].

During the next year a new U-OWC plant will be constructed in the Port of Salerno (Italy). Herein, we provide an overview on the crucial characteristics of the plant. Specifically, section II describes the plant and its deployment in the port layout; section III describes the expected performance of the system in realistic sea states by utilizing model developed and validated in the current scientific literature; and then conclusions are drawn about the future development of the plant.

1796 - WDD

F. Arena is with Natural Ocean Engineering Laboratory, DICEAM Dept., Mediterranean University of Reggio Calabria, Via Graziella 1, Loc. Feo di Vito, Reggio Calabria, Italy, 89122 (e-mail: arena@unirc.it) and with Wavenergy.it – Academic Spin-Off of the Mediterranean University.

A. Romolo is with Natural Ocean Engineering Laboratory, DICEAM Dept., Mediterranean University of Reggio Calabria, Via Graziella 1, Loc. Feo di Vito, Reggio Calabria, Italy, 89122 (e-mail: aromolo@unirc.it) and with Wavenergy.it – Academic Spin-Off of the Mediterranean University.

G. Malara is with Natural Ocean Engineering Laboratory, DICEAM Dept., Mediterranean University of Reggio Calabria, Via Graziella 1, Loc. Feo di Vito, Reggio Calabria, Italy, 89122 (e-mail: giovanni.malara@unirc.it).

V. Laface is with Natural Ocean Engineering Laboratory, DICEAM Dept., Mediterranean University of Reggio Calabria, Via Graziella 1, Loc. Feo di Vito, Reggio Calabria, Italy, 89122 (e-mail: valentina.laface@unirc.it).

E. Valentino is with the Port Authority of Salerno, via Roma, 29, 84121, Salerno, Italy (e-mail: e.valentino@porto.salerno.it).

F. Messina is with the Port Authority of Salerno, via Roma, 29, 84121, Salerno, Italy (e-mail: f.messineo@porto.napoli.it).

## II. PROJECT LAYOUT: PROJECT OF THE NEW U-OWC FOR SALERNO'S HARBOUR

The U-OWC described in this article will be installed in the Port of Salerno, which is located in the South of the Italian peninsula in front of the Tyrrhenian Sea. The actual layout of the port is shown in Fig. 1. The whole infrastructure has an area of 1,7 km<sup>2</sup>, where 500.000 m<sup>2</sup> are reserved for ground area. The connection with the open sea is established via a 280 m wide port entrance in a water depth of 13 m, while the turning basin diameter is 550 m in a water depth of 12 m. The port has 9 quays with an overall length of 2.950 m in a water depth of 11.8 m and 16 berths on 5 piers.

The breakwater protecting the inner basin is 1.550 m long on the East side, while the West side is protected by a 1.180 m long breakwater. The port has also an entrance on the East side, which is protected by a breakwater having a length of 350 m.

The port of Salerno plays a key role for the commercial growth of the region and, since 2011, is experiencing a growth in the number of arrived vessels (from 2.531 in 2011 to 2.807 in 2017) and in the total cargo handled (from 10.533.335 t in 2011 to 14.968.690 t in 2017).

The modified layout of the port infrastructure is shown in Fig. 2. It shows that the end of the West breakwater will be demolished for a length of about 100 m, while the East breakwater will be extended of about 180 m by adopting U-OWCs.

The plan view of the U-OWC breakwater is shown in Fig. 3 and Fig. 4. The breakwater will be composed by vertical caissons extending from the actual end towards the West direction. The new breakwater will include a round head with armour layers and three U-OWC caissons (the n° 2, 3 and 4 of Fig. 4). Each caisson will host ten independent chambers. The round head overlaps partially with the U-OWC breakwater, so that caisson n° 2 in Fig. 4 is only partially fully operative.

Fig. 5 shows the vertical cross-section of the structure at the centre of the breakwater. The structure embodies the wave energy converter on the wave beaten side and the ballasting infrastructure on the land side. The breakwater shown in the figure is installed on a water depth of about 13 m. The U-OWC embodied in the breakwater has a vertical duct 2 m wide and 8.60 m long with an opening located 2 m below the m.w.l., an inner chamber of 4 m, with an air chamber extending up to 6 m over the m.w.l. The air chamber has an orifice with a diameter of 0.8 m facing a secondary chamber, which is designed for serving as machinery room in case of installation of Power Take-Off systems. The width of the chambers in the transversal direction is 3.5 m (see Fig. 6). The global stability of the infrastructure is ensured via ballasts filled with sand. The connection between the U-OWCs and the other infrastructures is shown in Fig. 7, where it is seen that two traditional caissons are installed on the sides of the wave energy converters.

## III. MODEL OUTPUTS

This section describes numerical results obtained by theoretical models. The objective of this application is to evaluate the energy-wise performance of the system. Initially, the main characteristics of the mathematical model are described in conjunction with the equations used for estimating the power output of the system. Then, the numerical results are described.

### A. Model description

The model used in this numerical application was proposed by Boccotti [8]. It is based on the coupling between the unsteady Bernoulli equation and the equation of conservation of the air mass, which is further manipulated by assuming that the air is described by an isentropic process. Power outputs are calculated by considering that the U-OWCs are equipped with Wells turbines, which are commonly utilized in conjunction with OWC systems [6], [15].

Figure 8 shows the vertical cross-section of a U-OWC embodied in a vertical breakwater and its geometric characteristics. The device is installed in a constant water depth  $d$ , its opening has submergence  $h$  and width  $b_1$ , and the length of the vertical duct is  $l_i$ . The air chamber is  $b_2$  wide, with height  $h_c$  measured from the mean water level (m.w.l.). The instantaneous level of the free surface displacement of the water column  $\xi$  is positive downward and measured from the top of the air chamber. At the top of the air chamber is located the PTO. The diameter of the orifice, where the PTO will be installed, is  $D$ . In this analysis the transversal width  $b_3$  of the chamber (not shown in the figure) is assumed small compared to the incident wave length, so that the rigid piston model can be adopted for describing the water column oscillations.

In this context, the water column equation of motion is [8],

$$\frac{l_i}{g} \frac{s''}{s'} \ddot{\xi} + \frac{(l_i + h + h_c - \xi)}{g} \ddot{\xi} = h' - h'' - \Delta h_w, \quad (1)$$

where  $h'$  and  $h''$  are the energies per unit weight at the water column free surface and at the U-OWC inlet, respectively; and  $\Delta h_w$  is a term accounting for the head losses along the water column.

Specifically, the energies per unit weight are given by the equations

$$h' = h_c - \xi + \frac{1}{2g} \dot{\xi}^2 + \frac{p - p_{atm}}{\rho_w g}, \quad (2)$$

and

$$h'' = \frac{\Delta p}{\rho_w g}, \quad (3)$$

where  $g$  is the acceleration of gravity;  $p$  is the air pressure inside the pneumatic chamber;  $p_{atm}$  is the atmospheric pressure;  $\rho_w$  is the water density; and  $\Delta p$  is the wave

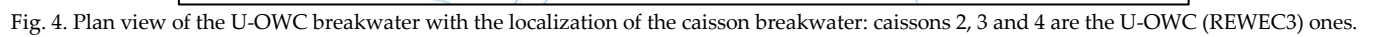
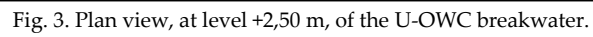


Fig. 1. View of the Salerno's harbor before the project of enlargement of 200m by the adoption of REWEC3 caisson breakwaters (Source: GoogleEarth).



Fig. 2. Introduction of the U-OWC (REWEC3) breakwaters in the actual layout of the Port of Salerno.







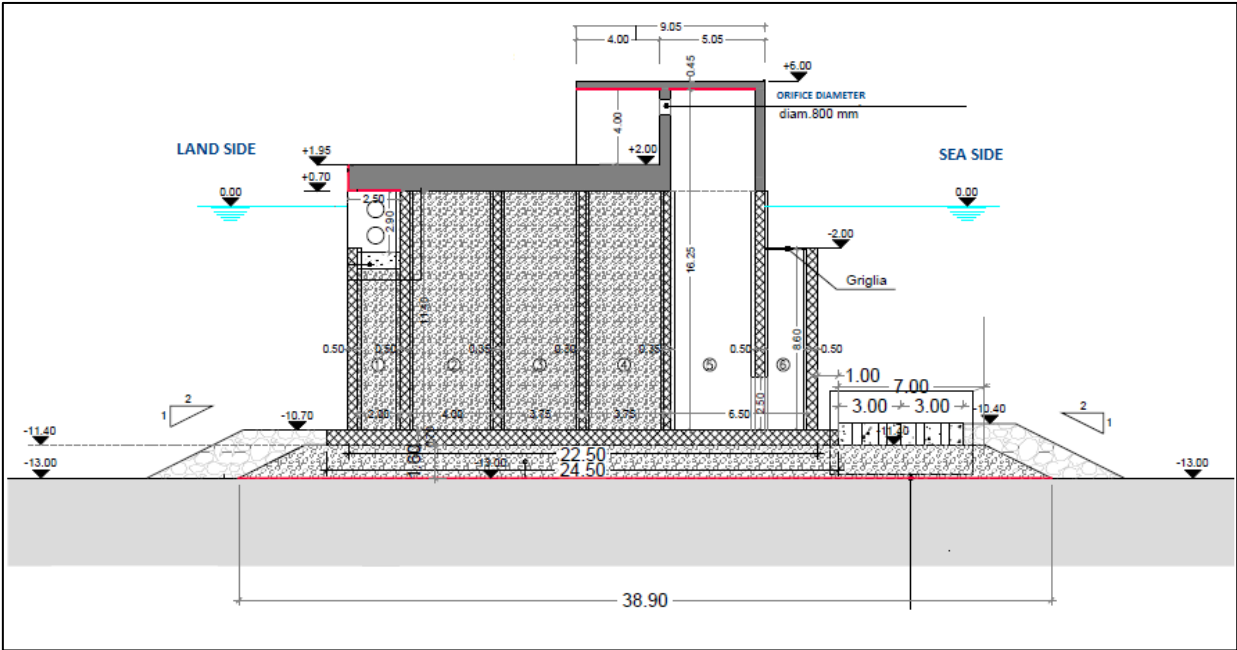


Fig. 5. Cross-section of a REWEC3 caissons (the 2, 3 and 4 of Fig. 4) in the Salerno's project, at the center of the breakwater.

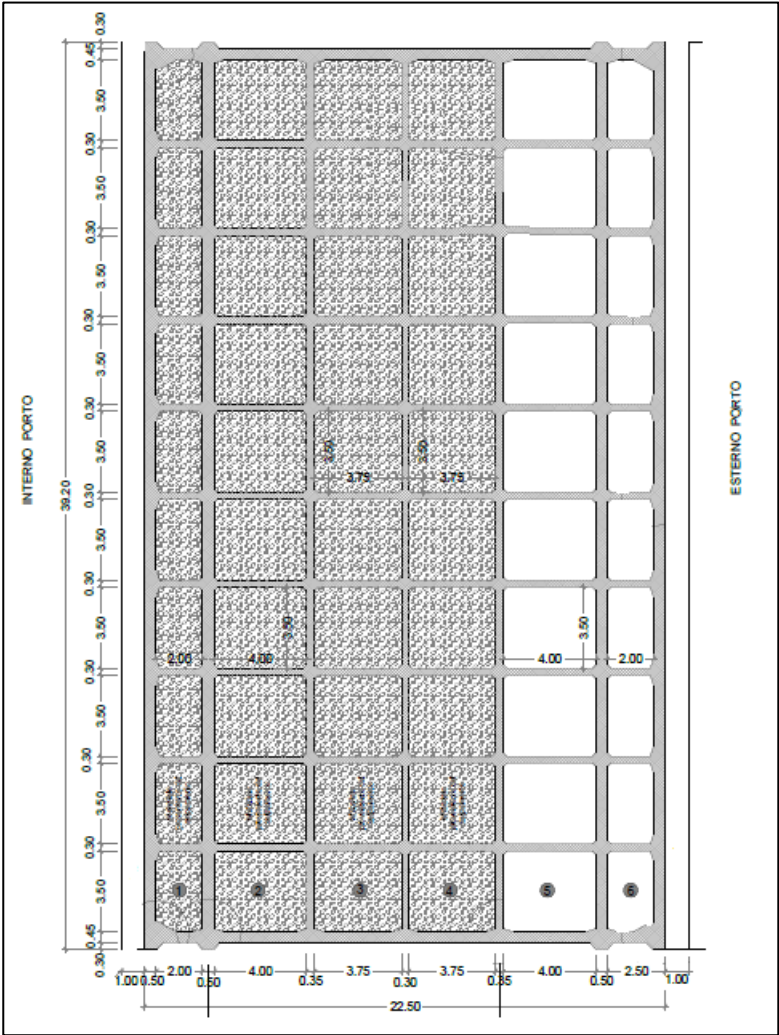


Fig. 6. Plant of a REWEC3 caisson in the Salerno's project.

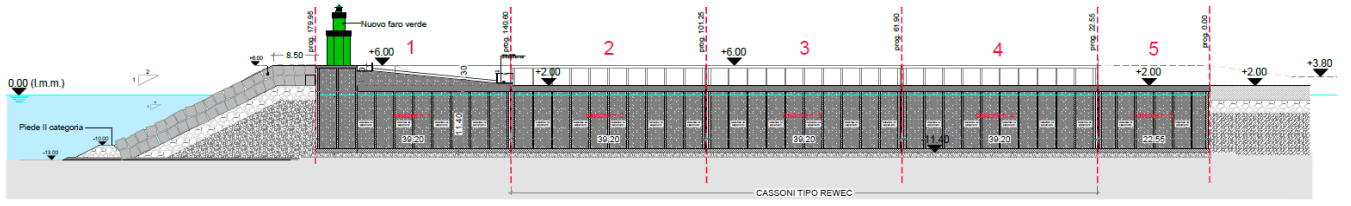


Fig. 7. Longitudinal-section of a REWEC3 caisson in the Salerno's project.

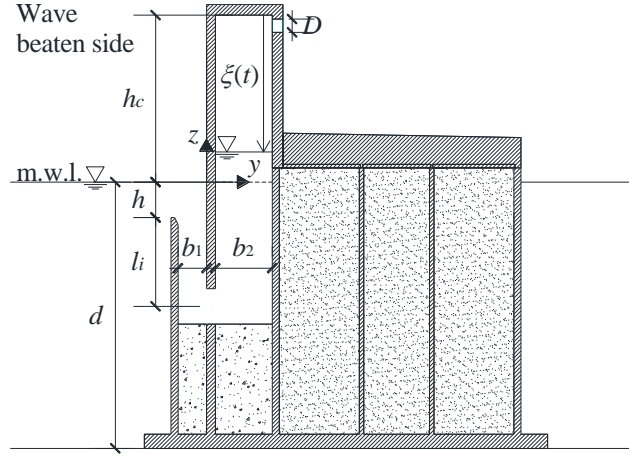


Fig. 8. Reference sketch of a U-OWC plant embodied in a vertical breakwater.

pressure at the inlet [8], [16].

In eq. (1), the head losses are accounted for by the methods described in Ref. [8]. The reliability of this model was fully verified by Boccotti [8] and by Malara *et al.* [17] via small scale field experiments and by Arena *et al.* [13], [14], [18] via comparison against full-scale data.

The water column equation of motion is coupled with the air mass conservation principle. Denoting the mass flow rate of air through the turbine as  $\dot{m}_{turb}$  (which is positive for outward flow), it is seen that the resulting equation is

$$-\dot{m}_{turb} = \rho \dot{V}_c + V_c \dot{\rho}, \quad (4)$$

where  $\rho$  is the air density inside the pneumatic chamber, and  $V_c$  is the instantaneous volume of the air in the chamber, which is calculated by the equation

$$V_c = b_2 b_3 \xi. \quad (5)$$

The compression/expansion of the air in the chamber is described under the assumption of isentropic process, so that

$$p = p_{atm} \frac{\rho^\gamma}{\rho_{atm}^\gamma}, \quad (6)$$

where  $\rho_{atm}$  is the atmospheric density, and  $\gamma$  is the specific heat ratio.

Defining the dimensionless relative pressure oscillation inside the chamber as:

$$p^* = \frac{p}{p_{atm}} - 1, \quad (7)$$

equations (4) and (6) yield to

$$\dot{p}^* = -\gamma(p^* + 1) \frac{\dot{V}_c}{V_c} - \gamma(p^* + 1)^\beta \frac{\dot{m}_{turb}}{\rho_{atm} V_c}, \quad (8)$$

with:

$$\beta = \frac{\gamma - 1}{\gamma}. \quad (9)$$

Thus, from Eq. (8), the mass flow rate of air through the turbine can be calculated as

$$\dot{m}_{turb} = - \left( \frac{p}{p_{atm}} \right)^{1/\gamma} \rho_{atm} b_2 b_3 \left[ \dot{\xi} + (h_c + \xi) \frac{1}{\gamma p} \dot{p} \right]. \quad (10)$$

In this work, the air flow rate is calculated by the equation

$$\dot{m}_{turb} = \frac{\Lambda D}{N} (p - p_{atm}), \quad (11)$$

$\Lambda$  being a dimensionless turbine coefficient,  $N$  being the turbine rotational speed and  $D$  being the turbine outer diameter. Note that eq. (11) is valid for the Wells turbine air flow – pressure drop relation only. Otherwise other relations must be used [6].

## B. Numerical results

A prospect on the performance of the system is provided in this section. The presented numerical results are derived via Monte Carlo simulations. The simulations were run by generating sea states compatible with JONSWAP – Mitsuyasu directional spectra [19,20], which are used for synthesizing the time histories of the exciting wave pressure. Then, the equations of motion described in section III.A are integrated numerically via a finite-difference scheme. In all cases the U-OWC is supposed equipped with a monoplane Wells turbine having the characteristics described by Curran and Gato [15] and rotating at constant speed. The response time histories are post-processed for estimating the response statistics and the average power absorbed by the system.

The input wave data are determined by utilizing the nearshore wave data obtained by the buoy of Ponza of the RON (Rete Ondametrica Nazionale – Italian Buoy Network) and propagated to the opening of the Port. Figure 9 shows the frequencies of occurrence of the seastates recorded near the port area. By integrating this information with the average incident wave power

propagated by these sea states, the following two sea states are identified for the numerical simulations:

- sea state 1 with  $H_s = 2$  m and  $T_p = 6$  s;
- sea state 2 with  $H_s = 2.5$  m and  $T_p = 7$  s.

These sea states are selected as they propagate a relevant fraction of the average annual incident wave energy.

Examples of time histories generated in these cases are shown in Fig. 10 and Fig 11. Note that the figures show a small portion of the complete time histories. Indeed, in both cases,  $10^6$  samples were generated. Such a number of samples was selected in order to estimated reliably the probability density function of the response components. These results are shown in Fig. 12 and Fig. 13. It is seen that the response distributions may deviate slightly from the Gaussian distribution. Further, the distribution shape may change depending on the sea state intensity. This fact relates to the characteristics of the adopted theoretical model and, specifically, on the included nonlinear terms. From an energy wise perspective, these two numerical examples emphasize the fact that at different conditions, different performances may be observed. Indeed, the U-OWC absorbed 80% of the incident energy in sea state 1 and 61% in sea state 2.

#### IV. CONCLUSIONS

This article has provided an overview on the critical characteristics of the U-OWC plant that will be constructed in the Port of Salerno (Italy). The plant will be composed by three caissons which are used for extending the basin of the actual port. The performance of this plant will be further examined in the future development of this work. Specifically, after the construction of the infrastructure, the plant will be equipped with an

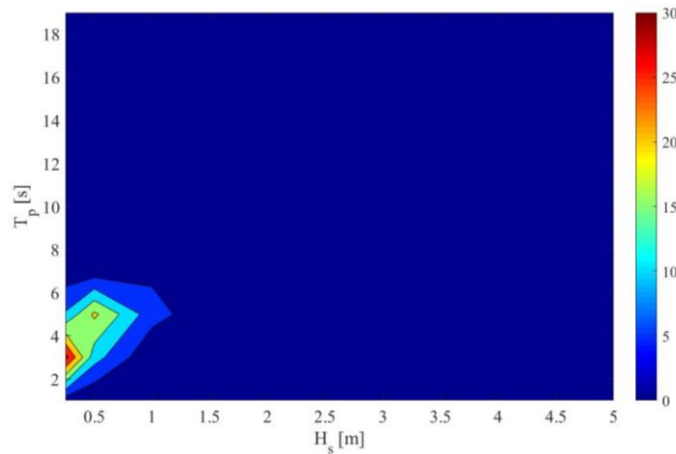


Fig. 9. Frequencies of occurrence of sea states with given significant wave height ( $H_s$ ) and peak spectral period ( $T_p$ ).

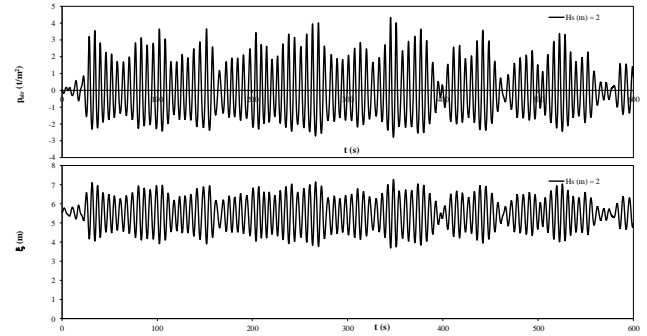


Fig. 10. Time histories of the air pressure (upper panel) and of the water column displacement (lower panel) associated with sea state 1.

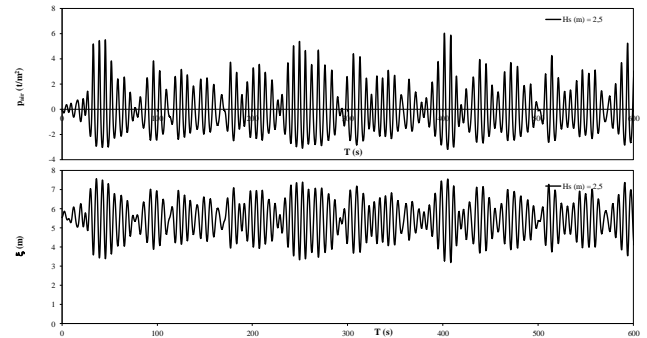


Fig. 11. Time histories of the air pressure (upper panel) and of the water column displacement (lower panel) associated with sea state 2

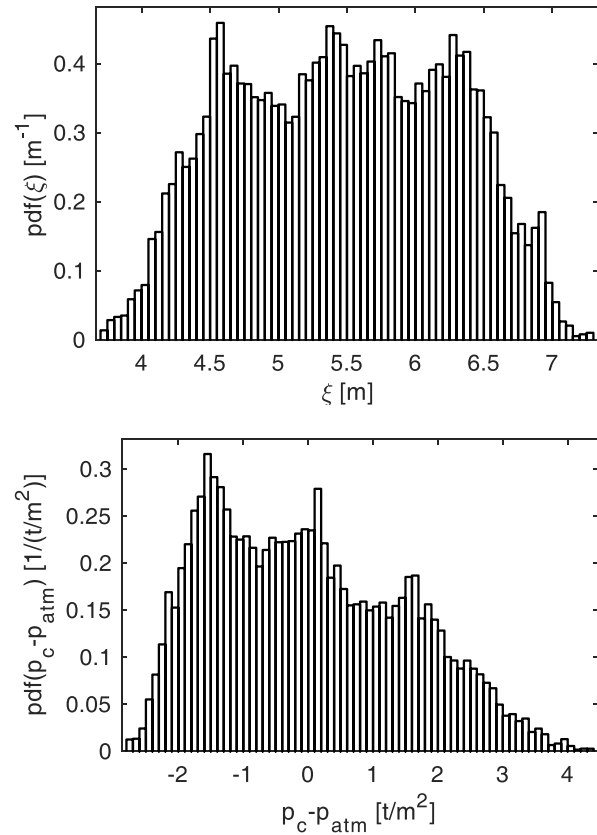


Fig. 12. Probability density function of the water column displacement (upper panel) and of the air pressure (lower panel) associated with sea state 1.



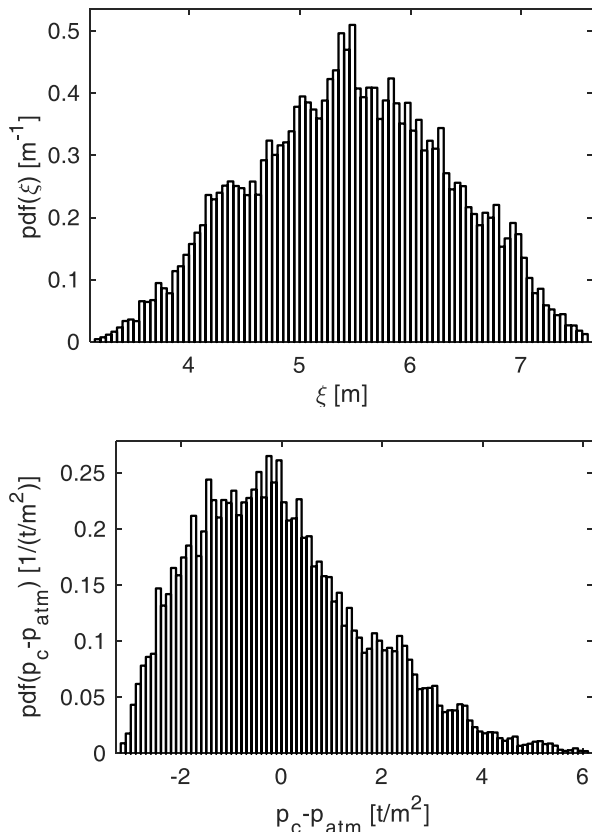


Fig. 13. Probability density function of the water column displacement (upper panel) and of the air pressure (lower panel) associated with sea state 2.

adequate Power Take Off (PTO) system. For this purpose, studies devoted to the identification of the best technological option will be undertaken.

#### ACKNOWLEDGEMENT

We thank ACMAR company for providing the technical drawings.

#### REFERENCES

- [1] H. Hotta, T. Miyazaki, Y. Washio, S.I. Ishii, On the performance of the wave power device Kaimei - the results on the open sea tests, in: Proc. 7th Int. Conf. Offshore Mech. Arct. Eng. - OMAE1988, Houston, U.S.A., 1988: pp. 91–96.
- [2] Y. Masuda, An experience of wave power generator through tests and improvement, in: D. V. Evans, A.F. de O. Falcão (Eds.), Falcão A.F. O., Evans D.V., Editors. Hydrodyn. Ocean Wave-Energy Util., Springer Berlin Heidelberg, Berlin, Heidelberg, 1986: pp. 445–452. doi:10.1007/978-3-642-82666-5.
- [3] M. Ravindran, P.M. Koola, Energy from sea waves—the Indian wave energy program, Curr. Sci. 60 (1991) 676–80. doi:10.2307/24093688.
- [4] A.F. de O. Falcão, The shoreline OWC wave power plant at the Azores, in: Proc. 4th Eur. Wave Energy Conf., Aalborg, Denmark, 2000: pp. 42–48.
- [5] T. Healt, T.J.T. Whittaker, C.B. Boake, The design, construction and operation of the LIMPET wave energy converter (Islay, Scotland), in: Proc. 4th Eur. Wave Energy Conf. Aalborg, Denmark, Aalborg, Denmark, 2000: pp. 49–55.
- [6] A.F.O. Falcão, J.C.C. Henriques, Oscillating-water-column wave energy converters and air turbines: A review, Renew. Energy. 85 (2016) 1391–1424. doi:10.1016/j.renene.2015.07.086.
- [7] P. Boccotti, On a new wave energy absorber, Ocean Eng. 30 (2003) 1191–1200. doi:10.1016/S0029-8018(02)00102-6.
- [8] P. Boccotti, Caisson breakwaters embodying an OWC with a small opening—Part I: Theory, Ocean Eng. 34 (2007) 806–819. doi:10.1016/j.OCEANENG.2006.04.006.
- [9] F. Arena, A. Romolo, G. Malara, V. Fiamma, A Small Scale Field Experiment on a U-OWC, in: Proc. 10th Eur. Wave Tidal Energy Conf., Aalborg, Denmark, 2013: pp. 2–8.
- [10] F. Arena, G. Malara, A. Romolo, A U-OWC wave energy converter in the Mediterranean Sea: Preliminary results on the monitoring system of the first prototype, in: Guedes Soares (Ed.), Proc. 1st Int. Conf. Renew. Energies Offshore - RENEW2014, CRC Press, Lisbon, Portugal, 2014: pp. 417–421. doi:10.1201/b18973-59.
- [11] P. Boccotti, Comparison between a U-OWC and a conventional OWC, Ocean Eng. 34 (2007) 799–805. doi:10.1016/j.oceaneng.2006.04.005.
- [12] F. Arena, A. Romolo, G. Malara, A. Ascanelli, On Design and Building of a U-OWC Wave Energy Converter in the Mediterranean Sea: A Case Study, in: Proc. 32nd Int. Conf. Ocean. Offshore Arct. Eng., 2013: p. V008T09A102. doi:10.1115/omae2013-11593.
- [13] F. Arena, A. Romolo, G. Malara, V. Fiamma, V. Laface, The First Full Operative U-OWC Plants in the Port of Civitavecchia, in: Vol. 10 Ocean Renew. Energy, 2017: p. V010T09A022. doi:10.1115/OMAE2017-62036.
- [14] F. Arena, A. Romolo, G. Malara, V. Fiamma, V. Laface, Response of the U-OWC Prototype Installed in the Civitavecchia Harbour, in: Proc 37th Int. Conf. Offshore, Mech. Arct. Eng., Madrid, Spain, 2018: p. V010T09A034. doi:10.1115/OMAE2018-78762.
- [15] R. Curran, L.M.C. Gato, The energy conversion performance of several types of Wells turbine designs, Proc. Inst. Mech. Eng. Part A J. Power Energy. 211 (1997) 133–145. doi:10.1243/0957650971537051.
- [16] G. Malara, F. Arena, Response of U-Oscillating Water Column arrays: semi-analytical approach and numerical results, Renew. Energy. 138 (2019) 1152–1165. doi:10.1016/j.renene.2019.02.018.
- [17] G. Malara, A. Romolo, V. Fiamma, F. Arena, On the modelling of water column oscillations in U-OWC energy harvesters, Renew. Energy. 101 (2017) 964–972. doi:10.1016/j.renene.2016.09.051.
- [18] F. Arena, A. Romolo, G. Malara, V. Fiamma, V. Laface, Validation of the U-Oscillating Water Column model by full-scale experimental data, in: Proc. 12th Eur. Wave Tidal Energy Conf., Cork, Ireland, 2017.
- [19] K. Hasselmann, T.P. Barnett, E. Bouws, H. Carlson, D.E. Cartwright, K. Enke, J.A. Ewing, H. Gienapp, D.E. Hasselmann, P. Kruseman, A. Meerburg, P. Muller, D.J. Olbers, K. Richter, W. Sell, H. Walden, Measurements of Wind-Wave Growth and Swell Decay during the Joint North Sea Wave Project (JONSWAP), Ergnzungsh. Zur Dtsch. Hydrogr. Zeitschrift R. A(8) (1973) p.95.
- [20] H. Mitsuyasu, F. Tasai, T. Suhara, S. Mizuno, M. Ohkusu, T. Honda, K. Rikiishi, Observations of the Directional Spectrum of Ocean Waves Using a Cloverleaf Buoy, J. Phys. Oceanogr. 5 (1975) 750–760. doi:10.1175/1520-0485(1975)005<0750:OOTDSO>2.0.CO;2.